HHS Public Access

Author manuscript

Oncogene. Author manuscript; available in PMC 2016 August 10.

Published in final edited form as:

Oncogene. 2016 July 21; 35(29): 3880–3886. doi:10.1038/onc.2015.437.

Kras^{G12D} induces EGFR-MYC cross signaling in murine primary pancreatic ductal epithelial cells

Sandra Diersch[1,§], **Matthias Wirth**[1,§], **Christian Schneeweis**[1,§], **Simone Jörs**[1], **Fabian Geisler**[1], **Jens T. Siveke**[1,2], **Roland Rad**[1], **Roland M. Schmid**[1], **Dieter Saur**[1], **Anil K. Rustgi**[3,4,5,6], **Maximilian Reichert**[1,3,6], and **Günter Schneider**[1,*]

[1]II. Medizinische Klinik, Technische Universität München, München, 81675, Germany

[2]Division of Translational Solid Tumor Oncology, German Cancer Consortium (DKTK), partner site Essen and German Cancer Research Center (DKFZ), Heidelberg, Germany

[3]Division of Gastroenterology, Perelman School of Medicine, University of Pennsylvania, Philadelphia, PA 19104, USA

[4]Department of Medicine, Perelman School of Medicine, University of Pennsylvania, Philadelphia, PA 19104, USA

[5]Department of Genetics, Perelman School of Medicine, University of Pennsylvania, Philadelphia, PA 19104, USA

[6]Abramson Cancer Center, Perelman School of Medicine, University of Pennsylvania, Philadelphia, PA 19104, USA

Abstract

Epidermal growth factor receptor (EGFR) signaling has a critical role in oncogenic *Kras*-driven pancreatic carcinogenesis. However, the downstream targets of this signaling network are largely unknown. We developed a novel model system utilizing murine primary pancreatic ductal epithelial cells (PDECs), genetically engineered to allow time-specific expression of oncogenic *Kras^{G12D}* from the endogenous promoter. We show that primary PDECs are susceptible to Kras^{G12D}-driven transformation and form pancreatic ductal adenocarcinomas (PDAC) *in vivo* after *Cdkn2a* inactivation. In addition, we demonstrate that activation of Kras^{G12D} induces an EGFR signaling loop to drive proliferation. Interestingly, pharmacological inhibition of EGFR fails to

[*]Corresponding author: Günter Schneider, Technische Universität München, Klinikum rechts der Isar, II. Medizinische Klinik, Ismaninger Str. 22, 81675 Munich, Germany, Tel.: +498941406395, Fax: +498941404910, guenter.schneider@tum.de.
[§]These authors contributed equally to this work

Conflict of interest

The authors declare no conflict of interest.

Supplementary Information accompanies the paper on the Oncogene website (http://www.nature.com/onc)

Author Contributions

Concept and design of the research: S.D., M.W., C.S., S.J., F.G., M.R., R.M.S., D.S., A.K.R., G.S.; Realization of research: S.D., M.W., C.S., S.J., F.G., M.R.; Analysis and interpretation of data: all authors; Support with essential reagents/analytical tools: J.T.S., R.R., D.S., A.K.R.; J.T.S., F.G., D.S., M.R., A.K.R. and G.S. obtained funding; S.D., M.W., M.R. and G.S. wrote the paper. All authors discussed the results, commented on the manuscript, revised it critically for important intellectual content and approved the final version of the manuscript.

decrease $Kras^{G12D}$-activated ERK or PI3K signaling. Instead our data provide novel evidence that EGFR signaling is needed to activate the oncogenic and pro-proliferative transcription factor c-MYC. EGFR and c-MYC have been shown to be essential for pancreatic carcinogenesis. Importantly, our data link both pathways and thereby, explain the crucial role of EGFR for $Kras^{G12D}$-driven carcinogenesis in the pancreas.

Keywords

pancreatic cancer; EGFR; Kras; MYC

Introduction

Although novel chemotherapeutic regimens increased the overall survival of patients with advanced pancreatic ductal adenocarcinoma (PDAC), its prognosis remains dismal. The epidermal growth factor receptor (EGFR) signaling pathway plays an outstanding role in the carcinogenesis of the disease [1, 2]. Despite being active in only a subgroup of patients, the EGFR inhibitor erlotinib is currently the only known targeted therapeutic for PDAC. EGFR belongs to a receptor tyrosine kinase (RTK) family including ErbB2, ErbB3, and ErbB4[3]. Seven ligands, epidermal growth factor (EGF), transforming growth factor α (TGFα), betacellulin (BTC), heparin-binding EGF-like growth factor (HB-EGF), amphiregulin (ARG), epiregulin (EPR), and epigen (EGN) can induce receptor dimerization and consecutive activation [3]. Effectors acting downstream of EGFR in the $Kras^{G12D}$-induced circuit that drive tumor development in the pancreas remain incompletely understood.

In this study we generated a novel mouse model of PDAC, in which expression of the $Kras^{G12D}$ allele can be induced by a tamoxifen-inducible Cre recombinase in primary pancreatic ductal epithelial cells (PDECs). We provide evidence that $Kras^{G12D}$-driven proliferation of PDECs depends on an EGFR signaling loop engaging the oncogenic transcription factor c-MYC (MYC afterwards).

Results and Discussion

Mutations of the *Kras* oncogene are one of the earliest genetic events and have been shown to drive carcinogenesis in the pancreas [4]. To activate the expression of one allele of oncogenic $Kras^{G12D}$ from the endogenous gene promoter in PDECs, we isolated PDECs from $R26^{CreERT2};LSL\text{-}Kras^{G12D/+}$ mice (Fig. 1A). These cells show presence of ductal markers and the absence of acinar or endocrine markers (Fig. S1A). PDECs express genes associated with a progenitor state (Fig. S1A). Activation of the Cre recombinase in these cells by 4-hydroxytamoxifen (4-OHT) induced efficient recombination of the *Kras* locus (Fig. 1B) and more than 90% of the PDECs are recombined after 8 days of 4-OHT treatment (Fig. S1B–D). Expression of oncogenic $Kras^{G12D}$ induced GTP-bound Ras to an extent observed in murine $Kras^{G12D}$-driven PDAC cell lines (Fig. 1C). In addition, ERK becomes phosphorylated indicating activated canonical Kras signaling (Fig. 1D and 1E).

One road to PDAC originates in the pancreatic acinar cells likely via acinar-to-ductal metaplasia (ADM) and pancreatic intraepithelial neoplasia (PanIN) [5]. Although the

contribution of ductal cells to the carcinogenesis in the pancreas is still a matter of debate [6], available data suggest that ductal cells seem relatively refractory to $Kras^{G12D}$-driven transformation [7]. Therefore, we investigated whether PDECs can form PDAC *in vivo*. We orthotopically transplanted *ex vivo* tamoxifen-treated PDECs from *R26*^{CreERT2}*;LSL-Kras*$^{G12D/+}$ mice into the pancreas of immunodeficient mice. However, none of the transplanted mice (n=3) developed PDAC in the investigated time period of 51 days. Furthermore, we detected no pre-malignant lesions in the pancreas of these mice (Fig. S2A). In contrast, it has been reported that transplantation of PDECs, engineered to express $Kras^{G12D}$, into C57Bl/6 mice, leads to the formation of ductal structures resembling early PanIN lesions [8]. Considering low efficacy of $Kras^{G12D}$-dependent tumor initiation, the number of orthotopically transplanted PDEC cells (1×10^6 versus 0.15×10^6 cells) might account for this discrepancy. Indeed, after increasing the number of transplanted PDECs to 7.5×10^5 cells, formation of PanIN-like structures (lineage label [YFP] and keratin 19 [K19] positive) was detected (Fig. S2B). Besides activating mutations in the *Kras* gene, the tumor suppressor *Cdkn2a* is frequently lost in pre-neoplastic lesions. To model the human disease, we isolated PDECs from *R26*^{CreERT2}*;LSL-Kras*$^{G12D/+}$*;Cdkn2a*$^{lox/lox}$ mice (Fig. S2C). Tamoxifen treatment of these cells induced rapid loss of *p16*^{Ink4a} expression (Fig. S2D) and canonical $Kras^{G12D}$ signaling is activated (Fig. S2E). Orthotopic transplantation of *Cdkn2a*-deficient PDECs resulted in the development of invasive, proliferative, K19 positive, and metastatic PDAC (Fig. S2F–S2H). Thus, our model system suggests that PDECs contain a cellular population that is susceptible to $Kras^{G12D}$-induced transformation.

Expression of $Kras^{G12D}$ in PDECs induces proliferation (Fig. 2A and 2B) accompanied by induction of cell cycle genes, like *cyclin D1* or *cyclin A* (Fig. 2C). This is in agreement with observations that $Kras^{G12D}$ prevents premature senescence of PDECs [9] and induces a proliferative response [9–12].

In order to identify pathways driving $Kras^{G12D}$ induced proliferation, we used gene set enrichment analysis of mRNA expression profiles (GSEA). Several of the gene sets significantly enriched in $Kras^{G12D}$ expressing cells are linked to signatures controlled by the EGFR family (Fig. 2D and Supplemental Table 1). Accordingly, $Kras^{G12D}$ induced expression of the EGFR ligands amphiregulin and epiregulin (Fig. 2D and 2E), arguing for autocrine stimulation. Consistently, in murine PanIN organoids derived from ductal cells of *Pdx1-Cre;LSL-Kras*$^{G12D/+}$ mice [13], $Kras^{G12D}$ induced expression of EGFR ligands (Fig. S3). Along with upregulation of EGFR ligands, increased receptor auto-phosphorylation was observed (Fig. 2F). To test whether this EGFR phosphorylation is critical for mutant Kras-regulated proliferation we utilized the EGFR inhibitors erlotinib and gefitinib. Of note, in PDAC models, gefitinib has been demonstrated to be more specific for EGFR than erlotinib [14]. Both inhibitors diminished the $Kras^{G12D}$-induced EGFR phosphorylation (Fig. 2F) and decreased expression of cell cycle regulators, like cyclin D1 (Fig. 2G). A link between the EGFR loop and cyclin D1 was recently described in $Kras^{G12D}$-driven cancer formation in the pancreas *in vivo* [1]. Importantly, the $Kras^{G12D}$-mediated inactivation of the Rb-dependent restriction point in the G1-phase of the cell cycle is controlled by EGFR (Fig. 2G).

EGFR signaling networks engage ERK-, PI3K- and STAT3-controlled pathways. Although expression of oncogenic $Kras^{G12D}$ induced phosphorylation of ERK, AKT and its substrate GSK3β, both EGFR inhibitors did not distinctly change activation of these pathways (Fig. 3A and 3B). STAT3 phosphorylation was neither induced nor modulated by EGFR inhibitors (Fig. 3C). Involvement of EGFR in Ras induced transformation is context dependent [1, 2, 15] and the context appears to direct the signaling hubs engaged. Indeed, the hypomorphic waved-2 (wa2) EGFR receptor variant reduced AKT activation but not ERK phosphorylation in primary keratinocytes of K5-SOS-F mice [15]. In the pancreas, the EGFR-controlled signaling hubs are incompletely understood [16]. Despite expression of the $Kras^{G12V}$ oncogene, most acinar cells express low EGFR levels and nuclear phospho-AKT or phospho-STAT3 staining is absent [2]. Inflammatory stimuli increase EGFR expression and induce AKT and STAT3 phosphorylation in acinar cells in the context of oncogenic $Kras^{G12V}$ [2], arguing that AKT and STAT3 are part of the EGFR signaling network in this inflammatory context. Furthermore, EGFR signaling increased the signaling output of the canonical Kras pathway to induce acinar-to-ductal metaplasia (ADM) in $Kras^{G12D}$ expressing acinar cells [1]. In established Kras-driven PDAC models, the EGFR is inconsistently linked to active ERK, AKT or STAT3 [1, 2]. Together, these observations clearly demonstrate that the EGFR signaling network is modulated by cell-autonomous (e.g. tumor suppressor status) and non-autonomous (e.g. inflammatory environment) conditions.

The observation that ERK and AKT remain phosphorylated, despite an inactivation of EGFR auto-phosphorylation and cell cycle progression, suggests that different hubs sense the signal. To identify EGFR-engaged pathways, we again performed transcriptome profiling of EGFR inhibitor-treated PDECs. Enriched gene sets in $Kras^{G12D}$ expressing PDECs with an active EGFR loop were linked to the cell cycle, DNA replication and repair as well as anabolic pathways (Supplemental Table 2). Since we intended to identify an integration of the EGFR loop with the cell cycle machinery, we focused on transcription factors (TFT-MSigDB). We detected that the majority of EGFR-controlled gene sets were linked to the pro-proliferative E2F transcription factor family, corroborating the link of the EGFR loop to the cell cycle (Fig. 3D and Supplemental Table 3). Additionally, we observed six signatures associated with transcription factors of the MYC family (Fig. 3D, 3E, and Supplemental Table 3). Performing a GSEA with curated gene sets (C2) of the MSigDB revealed 18 significant MYC gene sets linked to EGFR (Supplemental Table 4). MYC adopts a prominent role in Ras-driven cancers [17–21]. Since MYC is strongly linked to the cell cycle of exocrine progenitors in the pancreas [22, 23] and to the E2F pathway in cell-based PDAC models [24], we investigated the role of MYC. First, we quantified mRNA levels of MYC target genes upon treatment with EGFR inhibitors. Both inhibitors reduced the expression of the MYC target genes *Ccna2, E2f1, eIf4e, Hspe1, Skp2, Ncl, and Odc1* (Fig. 3F), indicating robust cross signaling between EGFR and MYC. Second, to demonstrate the regulation of these genes by MYC in the context of murine PDECs, we used a novel dual-recombinase system, allowing the time-specific manipulation of genes [25]. We isolated murine PDECs at PanIN stages (2 months old mice) from *Pdx1-Flp;FSF-Kras$^{G12D/+}$;FSF-R26$^{CAG-CreERT2}$;R26$^{mT/mG}$;Myc$^{lox/lox}$* mice. We treated these PDECs for 24 hours with tamoxifen and sorted GFP expressing cells by FACS to investigate expression of MYC and its target genes. Here, *Myc* mRNA expression is reduced to 20% compared to untreated

controls, accompanied by a reduced mRNA expression of all investigated target genes (Fig. 3G).

Oncogenic activity of MYC is regulated by phosphorylation of threonine 58 and serine 62 residues at the N-terminal MYC homology box I [26, 27]. Indeed, mutant $Kras^{G12D}$ activation induces N-terminal phosphorylation of MYC (Fig. 4A). Increased MYC phosphorylation was detected over time (Fig. 4A and 4B). Furthermore, $Kras^{G12D}$ induces MYC protein expression (Fig. 4B), which is accompanied by a slight induction of *Myc* mRNA (Fig. 4C). Both EGFR inhibitors prevent $Kras^{G12D}$-induced MYC protein expression (Fig. 4B) and significantly reduce *Myc* mRNA expression (Fig 4C). MYC regulation is controlled at multiple levels in PDAC [21]. How the EGFR loop is connected to MYC expression is currently unknown and awaits further investigations. Nevertheless, our results show that $Kras^{G12D}$ induces MYC expression, phosphorylation, and MYC target gene expression in an EGFR-dependent manner, suggesting that the $Kras^{G12D}$-induced EGFR network is engaging MYC as an important effector.

Acinar cells cultured in suspension dedifferentiate and activate a ductal gene expression program [5, 28]. Therefore, the possibility exists that our PDEC preparations contain dedifferentiated acinar cells. However, in our hands, we were never able to serial passage and subculture acinar cells. This is in agreement with observations that *ex vivo* acinar cells lack the capacity to proliferate due to a p53-dependent growth arrest [29]. Since we subculture and serial passage the PDEC lines (only passage 3 to 8 were used for all experiments), a contamination with acinar cells is unlikely. To further address this point, lineage tracing technology using the ductal marker *Hnf1b-Cre^{ER}* mouse line was used [30] (Fig. 4D). First, we activated Cre recombinase in a *Hnf1b-Cre^{ER};LSL-Kras$^{G12D/+}$;R26^{Tom}* mouse by the i.p. application of tamoxifen *in vivo* [31]. Two weeks after the last tamoxifen administration we isolated PDECs. 87% of these cells express the reporter gene tdTomato (Fig. S4A), arguing for the ductal origin of the prepared cells. To further corroborate the EGFR-MYC loop in the *Hnf1β*-lineage, we isolated PDEC lines from untreated *Hnf1b-Cre^{ER};LSL-Kras$^{G12D/+}$;R26^{Tom}* mice. We adapted the tamoxifen treatment regime since 0.5 μM 4-OHT insufficiently recombined the *Kras* locus in *Hnf1b-Cre^{ER}* PDEC lines (Fig. S4B). Even upon an increased 4-OHT dose, only 54% of the cells expressed tdTomato after 7 days (Fig. S4C). However, the fraction of tdTomato expressing cells was increased to 91% after 15 days (Fig. S4D). Then the *Kras* locus is recombined (Fig. S4E) and the canonical Ras-pathway is activated (Fig. 4E). Additionally to ERK phosphorylation, the EGFR becomes phosphorylated, MYC protein and mRNA expression is induced and the G1-phase restriction point becomes inactivated upon the expression of $Kras^{G12D}$ (Fig. 4E and Fig. 4F). Both EGFR inhibitors prevent EGFR and Rb phosphorylation as well as MYC expression whereas ERK phosphorylation is not influenced (Fig. 4E and Fig. 4F). Together, the lack of proliferation of acinar cells *ex vivo* and our lineage tracing experiments argue that the described pathway and biology acts in the ductal lineage.

To further demonstrate the impact of the EGFR-dependent loop towards the proliferative capacity of $Kras^{G12D}$ expressing *Hnf1b-Cre^{ER};LSL-Kras$^{G12D/+}$;R26^{Tom}* PDECs, we measured growth of erlotinib- and gefitinib-treated cells. Both EGFR inhibitors reduce proliferation with a similar potency (Fig. 4G). To compare the effects of the EGFR blockade

with the effects of a direct MYC inhibitor, we treated the cells with 10058-F4. This MYC inhibitor prevents the dimerization of MYC with MAX [32]. Similar to EGFR inhibitors, 10058-F4 reduces proliferation of $Kras^{G12D}$ expressing PDECs, supporting an important function of MYC downstream of the EGFR.

Overall, PDECs are a valid model to gain mechanistic insights into Kras-driven processes in a specific pancreatic context [6, 8–12, 33]. In addition, PDECs are a tool for genetic screening experiments [34]. A multipotent subpopulation of adult pancreatic ductal cells capable of reprogramming towards the endocrine lineage was recently described, arguing for a stem cell population in the ductal compartment [35]. Consistently, our observations demonstrate that PDECs express progenitor markers and are susceptible to $Kras^{G12D}$-dependent transformation. In agreement, a non-islet Pdx1-positive PDEC subpopulation in the adult pancreas with a stem-like phenotype was described, harboring tumorigenic and metastatic capacity upon the expression of $Kras^{G12D}$ [36, 37]. In line with our data, MYC activation by $Kras^{G12D}$ was observed in this model and MYC was linked to the evolution of pancreatic cancer cells with stem cell-like features and metastatic potential [36, 37]. In addition, we analyzed recently published microarray datasets generated from duct and duct-like cells of *Pdx1-Cre;LSL-Kras*$^{G12D/+}$ mice [38] at pre-malignant disease stages. Indeed, we observed $Kras^{G12D}$-induced EGFR- and MYC-signatures using gene set enrichment analysis (Fig. S5), suggesting that the molecular changes occurring *in vivo* are recapitulated by our *in vitro* model. Furthermore, our data show that an EGFR-loop contributes to $Kras^{G12D}$-driven proliferation of PDECs, well in line with recent data from Kras-dependent mouse models [1, 2].

In addition to this EGFR loop, a $Kras^{G12D}$-activated autocrine loop engaging the insulin like growth factor 1 receptor (IGF1R) in *Cdnk2a/Trp53*-double deficient PDECs has recently been described [11]. Whether EGFR- and IGF1R-dependent loops act in parallel to modulate signaling thresholds and whether the usage of such circuits is determined by tumor suppressive programs, awaits further analysis. However, *in vivo* findings indicate that the need of EGFR signaling to develop $Kras^{G12D}$-driven PDACs is bypassed in a p53-deficient background [1, 2], arguing that tumor suppressors determine the need of such loops.

In contrast to the requirement of EGFR for oncogenic Kras-induced pancreatic carcinogenesis, molecular hubs of the EGFR network are incompletely defined. Although the cooperation of Ras and MYC oncogenes to transform cells has been described in the last century [39] and many underlying molecular processes are known [40], our data link for the first time two essential components of Kras-driven transformation in a pancreatic pre-neoplasia equivalent model. Like the EGFR loop, MYC essentially contributes to the carcinogenesis in the pancreas [19–21, 41, 42]. Especially, in embryonic stem cell-based genetically engineered mouse models the distinct effect of MYC silencing on disease progression and tumor formation was recently demonstrated [19]. MYC is highly expressed in multipotent pancreatic progenitor cells [43] and can autonomously drive tumor initiation and progression in the pancreas [21, 44–46]. The EGFR ligand TGFα dramatically accelerates MYC-driven carcinogenesis in the pancreas *in vivo* [47], which is consistent with our observation of an EGFR-MYC cross signaling. Therefore, connecting EGFR to MYC underscores the importance of the EGFR network in the pancreatic carcinogenesis.

Supplementary Material

Refer to Web version on PubMed Central for supplementary material.

Acknowledgments

We thank Drs. S. Hingorani, I. Verma, D. Tuveson, H. Zeng, F. Costantini, T. Jacks, R. DePhino, J. Ferrer, I. de Alboran, and F. Alt for generating or providing mouse lines/plasmids. This work was supported by the Wilhelm-Sander Foundation [2012.084.1 to G.S.], Deutsche Forschungsgemeinschaft (DFG) [SCHN 959/1-2, SCHN 959/2-1 to G.S., GE2289/1 to F.G., SI 1549/2-1 to J.T.S., and SFB824 to G.S. and D.S.], Deutsche Krebshilfe [110908 to G.S., 111273 (Max-Eder Program) to M.R., and 109992 to J.T.S.] and NIH [NIH P30 DK050306 Center for Molecular Studies in Digestive and Liver Diseases (Molecular Pathology and Imaging, Molecular Biology/Gene Expression, Cell Culture, and Transgenic and Chimeric Mouse Cores) to M.R. and A.K.R. and the NIH R01 DK060694 to M.R. and A.K.R.]

References

1. Ardito CM, Gruner BM, Takeuchi KK, Lubeseder-Martellato C, Teichmann N, Mazur PK, et al. EGF receptor is required for KRAS-induced pancreatic tumorigenesis. Cancer Cell. 2012; 22:304–317. [PubMed: 22975374]
2. Navas C, Hernandez-Porras I, Schuhmacher AJ, Sibilia M, Guerra C, Barbacid M. EGF receptor signaling is essential for k-ras oncogene-driven pancreatic ductal adenocarcinoma. Cancer Cell. 2012; 22:318–330. [PubMed: 22975375]
3. Lemmon MA, Schlessinger J, Ferguson KM. The EGFR Family: Not So Prototypical Receptor Tyrosine Kinases. Cold Spring Harb Perspect Biol. 2014:6.
4. Eser S, Schnieke A, Schneider G, Saur D. Oncogenic KRAS signalling in pancreatic cancer. Br J Cancer. 2014; 111:817–22. [PubMed: 24755884]
5. Puri S, Folias AE, Hebrok M. Plasticity and dedifferentiation within the pancreas: development, homeostasis, and disease. Cell Stem Cell. 2015; 16:18–31. [PubMed: 25465113]
6. Reichert M, Rustgi AK. Pancreatic ductal cells in development, regeneration, and neoplasia. J Clin Invest. 2011; 121:4572–4578. [PubMed: 22133881]
7. Kopp JL, von Figura G, Mayes E, Liu FF, Dubois CL, Morris JPt, et al. Identification of Sox9-dependent acinar-to-ductal reprogramming as the principal mechanism for initiation of pancreatic ductal adenocarcinoma. Cancer Cell. 2012; 22:737–750. [PubMed: 23201164]
8. Pylayeva-Gupta Y, Lee KE, Hajdu CH, Miller G, Bar-Sagi D. Oncogenic Kras-induced GM-CSF production promotes the development of pancreatic neoplasia. Cancer Cell. 2012; 21:836–847. [PubMed: 22698407]
9. Lee KE, Bar-Sagi D. Oncogenic KRas suppresses inflammation-associated senescence of pancreatic ductal cells. Cancer Cell. 2010; 18:448–458. [PubMed: 21075310]
10. Morton JP, Mongeau ME, Klimstra DS, Morris JP, Lee YC, Kawaguchi Y, et al. Sonic hedgehog acts at multiple stages during pancreatic tumorigenesis. Proc Natl Acad Sci U S A. 2007; 104:5103–5108. [PubMed: 17372229]
11. Appleman VA, Ahronian LG, Cai J, Klimstra DS, Lewis BC. KRAS(G12D)- and BRAF(V600E)-induced transformation of murine pancreatic epithelial cells requires MEK/ERK-stimulated IGF1R signaling. Mol Cancer Res. 2012; 10:1228–1239. [PubMed: 22871572]
12. Zhang W, Nandakumar N, Shi Y, Manzano M, Smith A, Graham G, et al. Downstream of mutant KRAS, the transcription regulator YAP is essential for neoplastic progression to pancreatic ductal adenocarcinoma. Sci Signal. 2014; 7:ra42. [PubMed: 24803537]
13. Boj SF, Hwang CI, Baker LA, Chio II, Engle DD, Corbo V, et al. Organoid models of human and mouse ductal pancreatic cancer. Cell. 2015; 160:324–338. [PubMed: 25557080]
14. Conradt L, Godl K, Schaab C, Tebbe A, Eser S, Diersch S, et al. Disclosure of erlotinib as a multikinase inhibitor in pancreatic ductal adenocarcinoma. Neoplasia. 2011; 13:1026–1034. [PubMed: 22131878]

15. Sibilia M, Fleischmann A, Behrens A, Stingl L, Carroll J, Watt FM, et al. The EGF receptor provides an essential survival signal for SOS-dependent skin tumor development. Cell. 2000; 102:211–220. [PubMed: 10943841]
16. Perera RM, Bardeesy N. Ready, set, go: the EGF receptor at the pancreatic cancer starting line. Cancer Cell. 2012; 22:281–282. [PubMed: 22975369]
17. Soucek L, Whitfield J, Martins CP, Finch AJ, Murphy DJ, Sodir NM, et al. Modelling Myc inhibition as a cancer therapy. Nature. 2008; 455:679–683. [PubMed: 18716624]
18. Soucek L, Whitfield JR, Sodir NM, Masso-Valles D, Serrano E, Karnezis AN, et al. Inhibition of Myc family proteins eradicates KRas-driven lung cancer in mice. Genes Dev. 2013; 27:504–513. [PubMed: 23475959]
19. Saborowski M, Saborowski A, Morris JPt, Bosbach B, Dow LE, Pelletier J, et al. A modular and flexible ESC-based mouse model of pancreatic cancer. Genes Dev. 2014; 28:85–97. [PubMed: 24395249]
20. Walz S, Lorenzin F, Morton J, Wiese KE, von Eyss B, Herold S, et al. Activation and repression by oncogenic MYC shape tumour-specific gene expression profiles. Nature. 2014; 511:483–487. [PubMed: 25043018]
21. Hessmann E, Schneider G, Ellenrieder V, Siveke JT. MYC in pancreatic cancer: novel mechanistic insights and their translation into therapeutic strategies. Oncogene. 2015; doi: 10.1038/onc.2015.216
22. Bonal C, Thorel F, Ait-Lounis A, Reith W, Trumpp A, Herrera PL. Pancreatic inactivation of c-Myc decreases acinar mass and transdifferentiates acinar cells into adipocytes in mice. Gastroenterology. 2009; 136:309–319. e309. [PubMed: 19022256]
23. Nakhai H, Siveke JT, Mendoza-Torres L, Schmid RM. Conditional inactivation of Myc impairs development of the exocrine pancreas. Development. 2008; 135:3191–3196. [PubMed: 18715949]
24. Schild C, Wirth M, Reichert M, Schmid RM, Saur D, Schneider G. PI3K signaling maintains c-myc expression to regulate transcription of E2F1 in pancreatic cancer cells. Mol Carcinog. 2009; 48:1149–1158. [PubMed: 19603422]
25. Schönhuber N, Seidler B, Schuck K, Veltkamp C, Schachtler C, Zukowska M, et al. A next-generation dual-recombinase system for time- and host-specific targeting of pancreatic cancer. Nat Med. 2014; 20:1340–1347. [PubMed: 25326799]
26. Hann SR. Role of post-translational modifications in regulating c-Myc proteolysis, transcriptional activity and biological function. Semin Cancer Biol. 2006; 16:288–302. [PubMed: 16938463]
27. Vervoorts J, Luscher-Firzlaff J, Luscher B. The ins and outs of MYC regulation by posttranslational mechanisms. J Biol Chem. 2006; 281:34725–34729. [PubMed: 16987807]
28. Pinho AV, Rooman I, Reichert M, De Medts N, Bouwens L, Rustgi AK, et al. Adult pancreatic acinar cells dedifferentiate to an embryonic progenitor phenotype with concomitant activation of a senescence programme that is present in chronic pancreatitis. Gut. 2011; 60:958–966. [PubMed: 21193456]
29. Pinho AV, Rooman I, Real FX. p53-dependent regulation of growth, epithelial-mesenchymal transition and stemness in normal pancreatic epithelial cells. Cell Cycle. 2011; 10:1312–1321. [PubMed: 21490434]
30. Solar M, Cardalda C, Houbracken I, Martin M, Maestro MA, De Medts N, et al. Pancreatic exocrine duct cells give rise to insulin-producing beta cells during embryogenesis but not after birth. Dev Cell. 2009; 17:849–860. [PubMed: 20059954]
31. Jörs S, Jeliazkova P, Ringelhan M, Thalhammer J, Durl S, Ferrer J, et al. Lineage fate of ductular reactions in liver injury and carcinogenesis. J Clin Invest. 2015; 125:2445–2457. [PubMed: 25915586]
32. Yin X, Giap C, Lazo JS, Prochownik EV. Low molecular weight inhibitors of Myc-Max interaction and function. Oncogene. 2003; 22:6151–6159. [PubMed: 13679853]
33. Schreiber FS, Deramaudt TB, Brunner TB, Boretti MI, Gooch KJ, Stoffers DA, et al. Successful growth and characterization of mouse pancreatic ductal cells: functional properties of the Ki-RAS(G12V) oncogene. Gastroenterology. 2004; 127:250–260. [PubMed: 15236190]

34. von Burstin J, Diersch S, Schneider G, Reichert M, Rustgi AK, Schmid RM. Detection of Tumor Suppressor Genes in Cancer Development by a Novel shRNA-Based Method. Mol Cancer Res. 2015; 13:863–869. [PubMed: 25724428]
35. Sancho R, Gruber R, Gu G, Behrens A. Loss of Fbw7 reprograms adult pancreatic ductal cells into alpha, delta, and beta cells. Cell Stem Cell. 2014; 15:139–153. [PubMed: 25105579]
36. Ischenko I, Zhi J, Moll UM, Nemajerova A, Petrenko O. Direct reprogramming by oncogenic Ras and Myc. Proc Natl Acad Sci U S A. 2013; 110:3937–3942. [PubMed: 23431158]
37. Ischenko I, Petrenko O, Hayman MJ. Analysis of the tumor-initiating and metastatic capacity of PDX1-positive cells from the adult pancreas. Proc Natl Acad Sci U S A. 2014; 111:3466–3471. [PubMed: 24550494]
38. Reichert M, Takano S, von Burstin J, Kim SB, Lee JS, Ihida-Stansbury K, et al. The Prrx1 homeodomain transcription factor plays a central role in pancreatic regeneration and carcinogenesis. Genes Dev. 2013; 27:288–300. [PubMed: 23355395]
39. Land H, Parada LF, Weinberg RA. Tumorigenic conversion of primary embryo fibroblasts requires at least two cooperating oncogenes. Nature. 1983; 304:596–602. [PubMed: 6308472]
40. Wang C, Lisanti MP, Liao DJ. Reviewing once more the c-myc and Ras collaboration: converging at the cyclin D1-CDK4 complex and challenging basic concepts of cancer biology. Cell Cycle. 2011; 10:57–67. [PubMed: 21200143]
41. Skoudy A, Hernandez-Munoz I, Navarro P. Pancreatic ductal adenocarcinoma and transcription factors: role of c-Myc. J Gastrointest Cancer. 2011; 42:76–84. [PubMed: 21279552]
42. Mazur PK, Herner A, Mello SS, Wirth M, Hausmann S, Sanchez-Rivera FJ, et al. Combined inhibition of BET family proteins and histone deacetylases as a potential epigenetics-based therapy for pancreatic ductal adenocarcinoma. Nat Med. 2015; doi: 10.1038/nm.3952
43. Zhou Q, Law AC, Rajagopal J, Anderson WJ, Gray PA, Melton DA. A multipotent progenitor domain guides pancreatic organogenesis. Dev Cell. 2007; 13:103–114. [PubMed: 17609113]
44. Sandgren EP, Quaife CJ, Paulovich AG, Palmiter RD, Brinster RL. Pancreatic tumor pathogenesis reflects the causative genetic lesion. Proc Natl Acad Sci U S A. 1991; 88:93–97. [PubMed: 1986386]
45. Grippo PJ, Sandgren EP. Acinar-to-ductal metaplasia accompanies c-myc-induced exocrine pancreatic cancer progression in transgenic rodents. Int J Cancer. 2012; 131:1243–1248. [PubMed: 22024988]
46. Lin WC, Rajbhandari N, Liu C, Sakamoto K, Zhang Q, Triplett AA, et al. Dormant cancer cells contribute to residual disease in a model of reversible pancreatic cancer. Cancer Res. 2013; 73:1821–1830. [PubMed: 23467612]
47. Sandgren EP, Luetteke NC, Qiu TH, Palmiter RD, Brinster RL, Lee DC. Transforming growth factor alpha dramatically enhances oncogene-induced carcinogenesis in transgenic mouse pancreas and liver. Mol Cell Biol. 1993; 13:320–330. [PubMed: 8417334]
48. Ventura A, Kirsch DG, McLaughlin ME, Tuveson DA, Grimm J, Lintault L, et al. Restoration of p53 function leads to tumour regression in vivo. Nature. 2007; 445:661–665. [PubMed: 17251932]
49. Hingorani SR, Petricoin EF, Maitra A, Rajapakse V, King C, Jacobetz MA, et al. Preinvasive and invasive ductal pancreatic cancer and its early detection in the mouse. Cancer Cell. 2003; 4:437–450. [PubMed: 14706336]
50. Wirth M, Stojanovic N, Christian J, Paul MC, Stauber RH, Schmid RM, et al. MYC and EGR1 synergize to trigger tumor cell death by controlling NOXA and BIM transcription upon treatment with the proteasome inhibitor bortezomib. Nucleic Acids Res. 2014; 42:10433–10447. [PubMed: 25147211]
51. Muzumdar MD, Tasic B, Miyamichi K, Li L, Luo L. A global double-fluorescent Cre reporter mouse. Genesis. 2007; 45:593–605. [PubMed: 17868096]
52. de Alboran IM, O'Hagan RC, Gartner F, Malynn B, Davidson L, Rickert R, et al. Analysis of C-MYC function in normal cells via conditional gene-targeted mutation. Immunity. 2001; 14:45–55. [PubMed: 11163229]
53. Madisen L, Zwingman TA, Sunkin SM, Oh SW, Zariwala HA, Gu H, et al. A robust and high-throughput Cre reporting and characterization system for the whole mouse brain. Nat Neurosci. 2010; 13:133–140. [PubMed: 20023653]

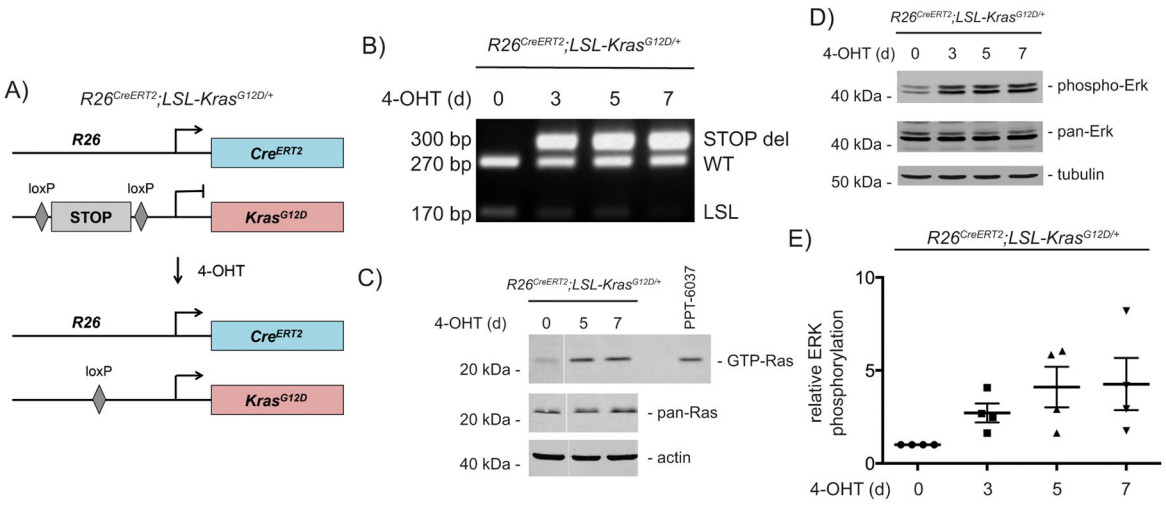

Figure 1. Activation of canonical Kras signaling in PDECs

A) Genetic strategy to activate Kras^{G12D}-expression in PDECs (*R26^{CreERT2};LSL-Kras$^{G12D/+}$*). Isolation of PDECs and mouse lines are described in detail in the supplementary material and methods section. All animal studies were conducted in compliance with European guidelines for the care and use of laboratory animals and were approved by the Institutional Animal Care and Use Committees (IACUC) of Technische Universität München, Regierung von Oberbayern, and the University of Pennsylvania. The *R26^{CreERT2}* mouse line was described in [48] and *LSL-Kras^{G12D}* line in [49]. B) Genotyping PCR of the indicated PDECs treated with 4-hydroxy-tamoxifen (4-OHT) (200 nM) (Sigma-Aldrich, München, Germany) over time. WT: wild type allele; LSL: *Lox-Stop-Lox* allele; STOP del: recombined LSL-allele. Primer sequences are depicted in the supplementary material and methods section. C) Ras pull-down assay (Raf-RBD Protein GST beads (Cytoskeleton, Denver, CO, USA)) from vehicle or 4-OHT (200 nM) treated PDECs. The murine Kras^{G12D}-driven PDAC cell line PPT-6037 was used as a positive control. Western blot of pan-Ras expression (clone 10, #05-516, Merck-Millipore, Darmstadt, Germany) (β-actin (Sigma-Aldrich): loading control) Irrelevant lanes were excised and the merger originated from the same gel. D) Western blot of phospho-ERK (Thr202/Tyr204) (#4370, Cell Signaling Technology, Danvers, MA, USA) and pan-ERK (#4696, Cell Signaling Technology) from vehicle or 4-OHT (200 nM) treated PDECs over the indicated time points (α-tubulin (Sigma-Aldrich): loading control). E) Quantification of ERK phosphorylation. PDECs from *R26^{CreERT2};LSL-Kras$^{G12D/+}$* mice were treated with 4-OHT (200 nM) over time. pan-ERK and phospho-ERK were determined in western blots and quantified using the Odyssey Infrared Imaging System (Li-Cor Biosciences, Bad Homburg, Germany), assuring measurements in the linear range. Shown is the relative ERK phosphorylation of four independent experiments using four individual PDEC lines.

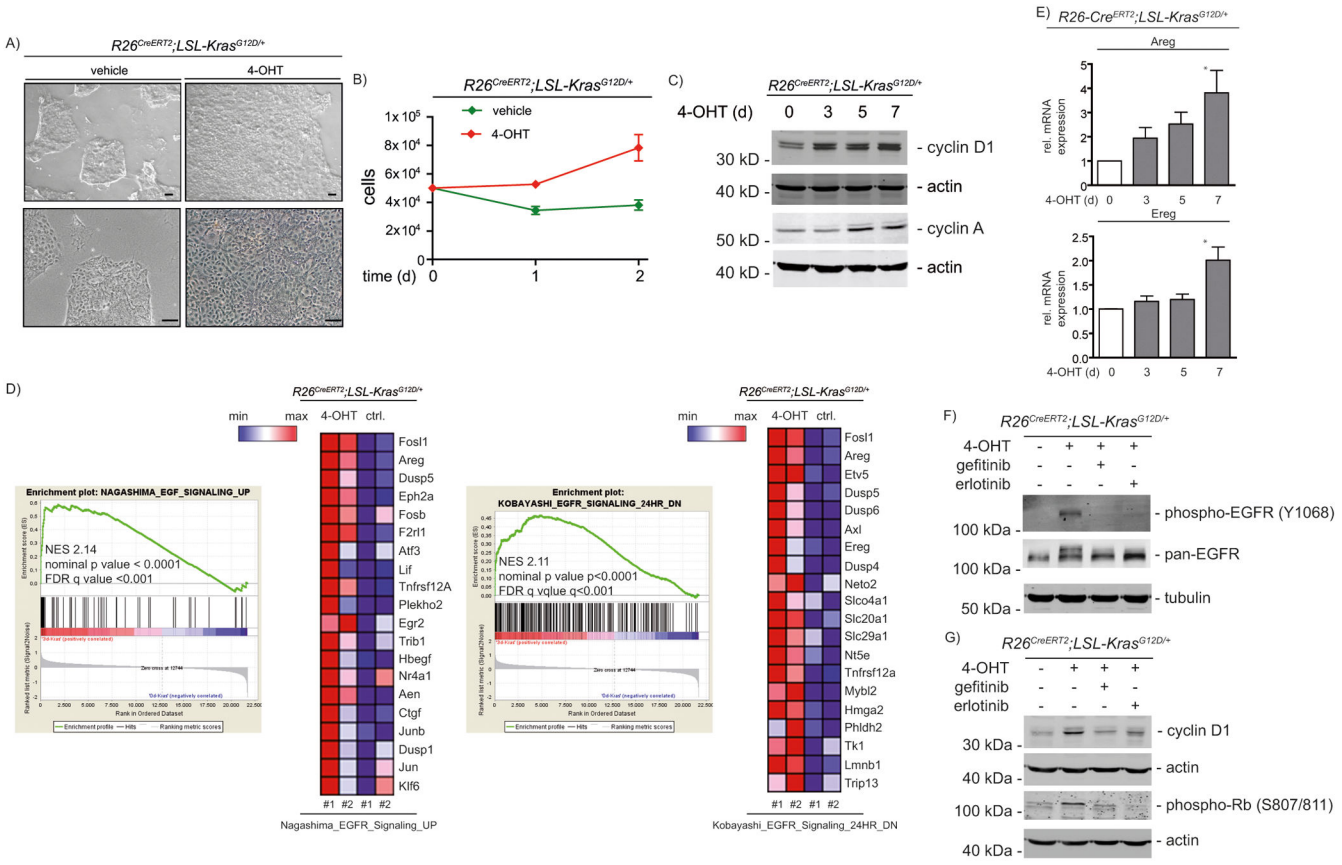

Figure 2. Kras^{G12D}-driven proliferation in PDECs depends on an EGFR-loop

A) White light microscopic images of PDECs from R26^{CreERT2};LSL-Kras$^{G12D/+}$ mice treated for five days with 200 nM 4-OHT or left as vehicle treated controls. Scale bars: 100 μm. B) PDECs from *R26^{CreERT2};LSL-Kras$^{G12D/+}$* mice were treated with 200 nM 4-OHT or were left as vehicle treated controls. After 7 days, 50.000 PDECs were seeded and cell number was determined for two additional days (two biological replicates performed as triplicates). C) PDECs from *R26^{CreERT2};LSL-Kras$^{G12D/+}$* mice were treated with 200 nM 4-OHT over time and cyclin D1 ((HD11), sc-246, Santa Cruz Biotechnology, Dallas, Tx, USA) and cyclin A ((H-432), sc-751, Santa Cruz Biotechnology) expression was measured in western blots. Different lysates were blotted to different membranes and loading was controlled by β-actin. D) Enrichment plots of EGFR signatures and corresponding heatmaps (top 20 EGFR controlled genes induced by Kras^{G12D}) from microarrays of vehicle (control: ctrl.) or 4-OHT (200 nM, 3 days) treated PDECs. NES: normalized enrichment score; FDR: false discovery rate. EMBL-EBI ArrayExpress Accession number: E-MTAB-2592. See supplementary material and methods for a description of the microarray analysis and gene set enrichment analysis. E) Relative *amphiregulin* (*Areg*) and *epiregulin (Ereg)* mRNA expression in 4-OHT (200 nM) treated PDECs was determined by qPCR using *cyclophilin A* mRNA expression as reference. Primers are depicted in supplementary material and methods. One way ANOVA *p-value < 0.05. F) and G) PDECs were treated for 6 days with 4-OHT (500 nM) and erlotinib or gefitinib (10 μM each; LC Laboratories, Woburn, MA, USA) were added for the last 24 hours as indicated. F) phospho-EGFR (#2234, Cell

Signaling Technology) and pan-EGFR ((1005), sc-03, Santa Cruz Biotechnology) western blot (α-tubulin: loading controls). G) cyclin D1 and phospho-Rb (#8516, Cell Signaling Technology) western blot. Different lysates were blotted to different membranes and loading was controlled by β-actin.

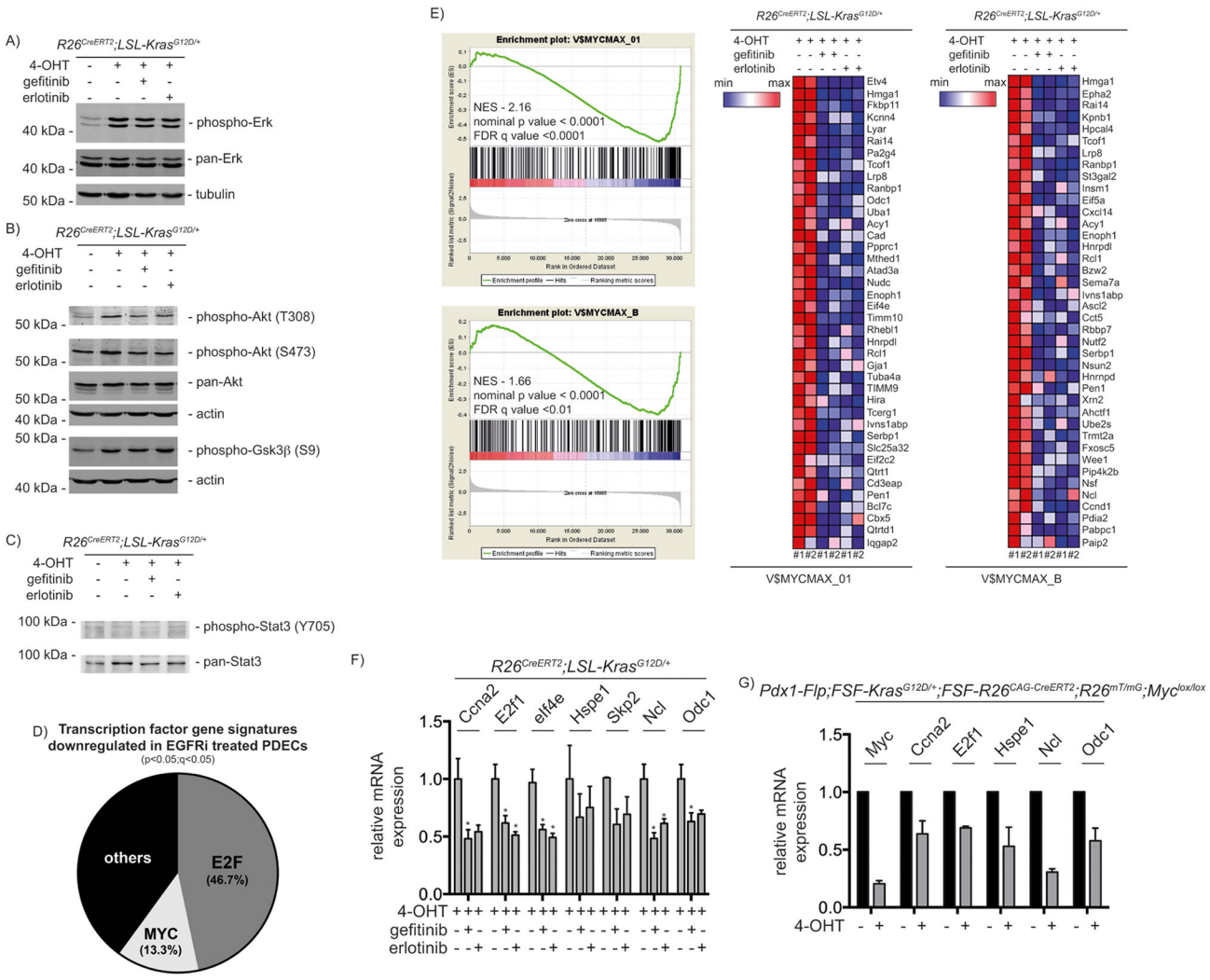

Figure 3. MYC is a downstream effector of EGFR

PDECs were treated for 6 days with 4-OHT (500 nM) and gefitinib or erlotinib (10 μM each) were added for the last 24 hours as indicated. Western blot of A) phospho- and pan-ERK (α-tubulin: loading controls). B) phospho-AKT (#9271 and #9275, Cell Signaling Technology) and -GSK3β (#9323, Cell Signaling Technology) as well as pan-AKT ((C67E7), #4691, Cell Signaling Technology). Different lysates were blotted to different membranes and loading was controlled by β-actin. C) phospho-STAT3 ((D3A7), #9145, Cell Signaling Technology) and pan-STAT3 ((C-20):sc-482, Santa Cruz Biotechnology) western blot. D) Transcription factor gene signatures (TFT-MSigDB) significantly downregulated in EGFR inhibitor (EGFRi) treated PDECs. PDECs were treated as described in A). E) GSEA enrichment plots of MYC signatures and corresponding heatmaps (top 40 MYC controlled genes inhibited by the EGFR inhibitors) from microarrays of PDECs treated as described in A). NES: normalized enrichment score; FDR: false discovery rate. EMBL-EBI ArrayExpress Accession number: E-MTAB-2592. See supplementary material and methods for a description of the microarray analysis and gene set enrichment analysis. F) PDECs were treated as described in A). Relative *Ccna2, E2F1, eIf4e, Hspe1, Skp2, Ncl,* and *Odc1*

mRNA expression levels were determined by qPCR using *beta-actin* mRNA expression as reference. Primers are depicted in supplementary material and methods. One way ANOVA *p-value < 0.05. G) PDECs from 2 months old *Pdx1-Flp;FSF-Kras$^{G12D/+}$;FSF-R26$^{CAG-CreERT2}$;R26$^{mT/mG}$;MYC$^{lox/lox}$* mice were isolated. In these cells expression of Kras^{G12D} is induced *in vivo* and expression of floxed genes can be manipulated by the treatment of cells with 4-OHT. The cells were treated with 4-OHT (500 nM) for 24 hours. The green fluorescent protein (GFP)-expressing cells were FACS (fluorescence-activated cell sorting) sorted as recently described [50]. Relative *Myc*, *Ccna2, E2f1, Hspe1, Ncl,* and *Odc1* mRNA expression levels were determined by qPCR using *beta-actin* mRNA expression as reference and compared to untreated cells, in which expression was set to 1. The *Pdx1-Flp, FSF-Kras^{G12D}, and the FSF-R26$^{CAG-Cre-ERT2}$* mouse lines were described recently in [25]. *The R26$^{mT/mG}$* mouse line is described in [51] and the *MYC^{lox}* line in [52].

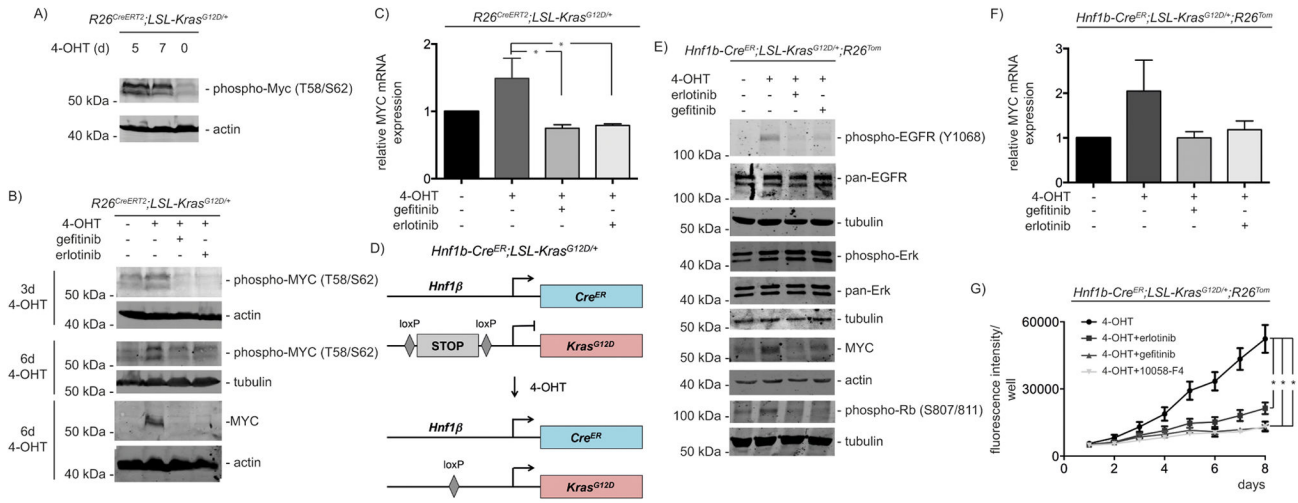

Figure 4. MYC expression is regulated by the autocrine EGFR-loop

A) Indicated PDECs were treated with 4-OHT (500 nM) over time. Western blot for phospho-MYC (#9401, Cell Signaling Technology) (β-actin: loading control). B) PDECs were treated with 4-OHT (500 nM) as indicated. Gefitinib or erlotinib (10 μM each) were added for the last 24 hours of incubation. Westernblot for phospho-MYC and MYC (#9402, Cell Signaling Technology). Different lysates were blotted to different membranes and loading was controlled by β-actin or α-tubulin as indicated. To detect phosphorylated MYC, PDECs were lysed by directly boiling in protein loading buffer. C) Indicated PDECs were treated with 4-OHT (500 nM) for 6 days. Gefitinib or erlotinib (10 μM each) were added for the last 24 hours of incubation. Relative *Myc* mRNA expression levels were determined by qPCR using *beta-actin* mRNA expression as reference. One way ANOVA *p-value < 0.05. D) Genetic strategy to activate $Kras^{G12D}$-expression in *Hnf1β*-positive PDECs (*Hnf1b-Cre^{ER};LSL-Kras$^{G12D/+}$;R26^{Tom}*). The *Hnf1b-Cre^{ER}* mouse line was described in [30] and the *R26^{Tom}* reporter mouse line in [53]. E) PDECs from *Hnf1b-Cre^{ER};LSL-Kras$^{G12D/+}$;R26^{Tom}* mice were treated with 4-OHT (1 μM) for 15 days. Afterwards gefitinib or erlotinib (10 μM each) were added for additional 24 hours or the cells were left as vehicle treated controls. Western blot of phospho-EGFR, pan-EGFR, phospho-ERK and pan-ERK, MYC, and phospho-Rb. Different lysates were blotted to different membranes and loading was controlled by β-actin or α-tubulin as indicated. F) PDECs from *Hnf1b-Cre^{ER};LSL-Kras$^{G12D/+}$;R26^{Tom}* mice were treated with 4-OHT (1 μM) for 15 days. Afterwards gefitinib or erlotinib (10 μM each) were added for additional 24 hours. Relative *Myc* mRNA expression levels were determined by qPCR using *beta-actin* mRNA expression as reference. G) PDECs from *Hnf1b-Cre^{ER};LSL-Kras$^{G12D/+}$;R26^{Tom}* mice were treated with 4-OHT (1 μM) for 15 days. Afterwards, 2.000 cells per well were seeded in a 96 well plate in quadruplicates (n=4). After 24 hours the cells were treated with erlotinib (10 μM), gefitinib (10 μM), or 10058-F4 (80 μM) or were left as vehicle treated controls. To determine relative growth, fluorescence (excitation: 560 nm, emission 590 nm) was measured daily over 8 days with a BMG FLUOstar OPTIMA Microplate Reader (BMG Labtech, Ortenberg, Germany). One way ANOVA *p-value < 0.05.